NUMERICAL ASSESSMENT OF BRICK WALLS' USE INCORPORATING A PHASE CHANGE MATERIAL TOWARDS THERMAL PERFORMANCE IN BUILDINGS DURING A PASSIVE COOLING STRATEGY

by

Zohir YOUNSI[a,b] and Hassan NAJI[b*]

[a] Yncréa-HEI, Univ. Artois, Univ. Lille, IMT Lille-Douai,
Laboratoire Génie Civil & géo-Environnement (*ULR 4515*), Technoparc Futura, F-62400 Béthune,
France 13 Rue de Toul, 59000 Lille, France
[b] Univ. Artois, Univ. Lille, IMT Lille-Douai & Yncréa-HEI,
Laboratoire Génie Civil & géo-Environnement (*ULR 4515*), Technoparc Futura,
F-62400 Béthune, France

Original scientific paper
https://doi.org/10.2298/TSCI180302207Y

The integration of new building materials incorporating phase change material (PCM) into the building envelope leads to an increase of the heat storage capacity, which may have an influence on minimizing the cooling demand and heating of the building. This work addresses a thermal performance enhancement of brick walls with incorporated PCM. The improvement has been assessed through a numerical approach in dealing with a 1-D transient conduction problem with phase change, while leaning on experimental results from a transient guarded hot plates method. The simulations have been fulfilled using a hybrid method combining both the finite volume method and an enthalpy porosity technique. The results of this combined approach are in good agreement. In the light of the findings obtained, it appears that PCM incorporation into a brick masonry can both reduce peak temperatures up to 3 °C and smooth out daily fluctuations. Thereby, the evaluation achieved can turns out useful in developing brick walls with an incorporated PCM for passive cooling, thus improving buildings thermal performance.

Key words: *PCM, masonry brick, composite wall, passive cooling, finite volumes, enthalpy method*

Introduction

Population growth and rapid economic development worldwide in recent decades have led to a rapid rise in energy demand. Thereby, in recent years many researchers around the world have worked out on finding innovative, efficient and cost-effective technology that can be used to reduce energy consumption in buildings, toward a sustainable energy future. In this context, many solutions are being implemented, including latent heat storage systems using PCM hereafter [1]. These are materials that, during a melting/solidification process at a constant or nearly constant temperature, absorb/release thermal energy from/to the surrounding space while avoiding overheating of the building components in which they are contained. They are widely used in management and energy storage fields, smart conditioning, solar cooling systems, energy storage for buildings, thermal comfortable textile design, to name a few. Thereby,

* Corresponding author, e-mail: hassane.naji@univ-artois.fr

PCM incorporation into building components has become a potential method of increasing thermal inertia with low volume, which improves energy buildings' efficiency by absorbing and storing the incoming solar radiation in the building envelope during the daytime while reducing indoor temperature swings [2]. Likewise, the PCM integration in building structures has become a very up-to-date topic. Note that PCM can be integrated into building materials in various ways [3-6]: either by direct incorporation, or impregnation, or manufacture of new panels with PCM to substitute conventional wallboards, or by incorporation of PCM capsules. Thus, the PCM must be thoroughly sealed inside cavities before being used in building elements to prevent the product's leakage during the melting process. It should be to point out that the PCM micro-encapsulation technology is increasingly used because of its ability to avoid leakage and to prevent forthright contact between the PCM and the building material. Although much researches have been conducted in recent years on such a topic [7-11], works on PCM incorporation in building bricks have been seldom addressed, yet widely used in mediterranean countries. Wherefore, this study aims to demonstrate the PCM integration concept in these typical constructions.

Even if the evaluation of the PCM effectiveness is mainly experimental, it can also be performed via numerical simulation [12-17] from a model that can be 1-D or 2-D or 3-D depending on the case to be dealt. On this subject, Zwanzig *et al* [12] developed a finite volume-based model to solve 1-D transient heat transfer through multi-layered building envelope surfaces. Their results indicate that using of a PCM composite wall panel in a building envelope can substantially decrease the heating peak and cooling loads while successfully shifting their peak to last hours of the day. To reduce the cooling load using envelopes incorporating PCM, Lei *et al.* [18] implemented a 1-D model with sinusoidal temperature boundary conditions (BC) representing the diurnal cycle. They found that adding a PCM layer reduces heat gains by 21-32% year-round, and that a proper PCM selection with suitable phase-change temperatures seems critical. Still in the same context, Koo *et al.* [19] experimentally validated a simulation for a PCM wallboard to find the effects of the nominal mean phase change temperature, its range, and convection heat transfer coefficients. Silva *et al.* [20] investigated both experimentally and numerically the effect of incorporating a macro-encapsulated PCM into a brick enclosure. They showed that a PCM-strengthened building envelope mitigates the indoor space temperature swing and reduces the thermal amplitude from 10 °C to 5 °C.

The study conducted here focuses on the study of the energy performance of a cement mortar incorporating a micro-encapsulated PCM that has been added to a brick wall. To carry out this, an enthalpy-based model is used to numerically simulate the thermal behavior. Such a computational model includes latent heat effects as a source term and includes a technique to ensure that the velocity field vanishes in the solid region. In this method, the *mushy zone* is frequently modeled as a *pseudo* porous zone where the *liquid fraction* is considered. Such an approach can handle phase change problems involving a fixed temperature or a temperature range. Since phase change problems are arduous, the enthalpy-based approach is increasingly adopted when seeking to solve them numerically. The objective of this work is twofold: to implement such an approach while validating it by comparison with experimental results of the guarded hot plates method [7], and to demonstrate the potential incorporation of the PCM into as a passive solution by reducing peak temperatures and smoothing out daily fluctuations in indoor space, which, in turn, would save lot of cooling energy.

System description

The majority of the external envelope walls in mediterranean countries are commonly constructed with horizontal clay bricks. Thereby, we aim here to study the thermal characteristic improvement of such a brick wall via the micro-encapsulated PCM insertion on the outer face. In the preparation of the composite materials, the micro encapsulated PCM used is composed of Micronal® DS5001X microcapsules (a special paraffin wax mixture) having a high latent heat storage capacity (about 110 J/g) and without leakage in the liquid phase. Its melting temperature is of 26 °C, which is close to the average diurnal temperature adopted herein. Note that the PCM studied were designed for cooling applications. For the purpose of this study, three different wall samples are investigated, namely, a typical brick wall (without PCM) and two multilayered walls incorporating a micro-encapsulated PCM into external envelope (Mortar + PCM), in which one of them has an extruded polystyrene insulation layer (XPS). The first wall sample (W1) is composed of a mortar layer with a thickness of 2 cm and 10 cm of bricks. The second sample (W2) is similar to the previous one, but with the micro-encapsulated PCM incorporated in the mortar layer. Finally, the third sample (W3) is composed of a mixture layer (Mortar + PCM) with a thickness 2 cm and 10 cm of brick with 10 cm of external insulation (extruded polystyrene XPS). The wall samples' geometry and composition are shown in fig. 1. The physical properties of all materials considered here are gathered in tab. 1.

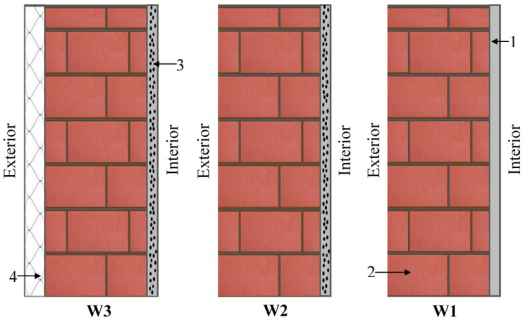

Figure 1. Wall samples' geometry and composition; *1 – mortar (2 cm), 2 – brick (10 cm), 3 – mortar-PCM (2 cm), 4 – XPS insulation (10 cm)*

Table 1. Thermophysical properties of various materials

Material	PCM DS5001X [7]	Mortar [21]	Brick [21]	XPS [21]
Solid's thermal conductivity [$Wm^{-1}K^{-1}$]	0.2	0.65	0.77	0.027
Liquid's thermal conductivity [$Wm^{-1}K^{-1}$]	0.13	–	–	–
Solid's heat capacity [$Jkg^{-1}K^{-1}$]	1700	925	835	1210
Liquid's heat capacity [$Jkg^{-1}K^{-1}$]	2153	–	–	–
Latent heat [$kJkg^{-1}$]	130	–	–	–
Densities [kgm^{-3}]	995	2001	1976	55

Numerical approach

This section deals with the mathematical modeling and the numerical solution approach for a PCM mortar-brick system. To cope with the problem of heat transfer with phase change in such a wall sample, the enthalpy-based method has been adopted. Specifically, the model is governed by the heat conduction equation incorporated with the enthalpy formation where latent heat of phase change and sensible heat are handled separately (see hereinafter).

Mathematical modeling

Before addressing the model equations, it should be recalled that the current research study deals with the transient heat transfer problem through multi-layered wall systems where

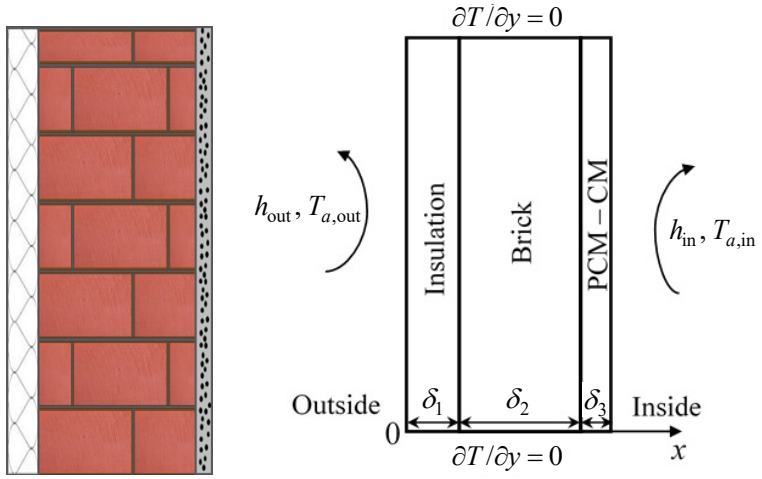

Figure 2. (a) A wall-PCM multi-layer depiction, (b) computed model along with BC, δ_1, δ_2, and δ_3 being the layers' thicknesses

a composite mortar-PCM is added in a conventional brick, fig. 2. Such a composite material is a mixture between a conventional building material (cement mortar) and very small particles of a micro-encapsulated PCM. However, despite these inclusions, the cement mortar remains as a homogeneous medium.

Before performing the numerical simulations via governing equations resolution, the following conjectures were made to simplify as follows: The heat transfer is 1-D, and end effects are neglected; All wall system layers are homogenous and isotropic; The microcapsules are uniformly distributed inside the mortar; The thermophysical properties are constant, although different in liquid and solid phases, densities, heat capacities and thermal conductivities are assumed to be time and temperature independent [7]; Horizontal walls are assumed to be insulated; Interfacial resistances are negligible; Natural convection and radiation heat transfer in the material are skipped; The melting point, freezing point and latent heat are constant.

Based on assumptions as previously stated, the mathematical model is set-up from the Fourier heat conduction equation for one dimension [22]:

$$\rho_i c_{P,i} \frac{\partial T}{\partial t} = \nabla\left(k_i \nabla T\right) \tag{1}$$

where T is the temperature, ρ – the density, k – the thermal conductivity, and c_P – the specific heat. Note that the subscript i denotes either the brick material, the thermal insulation or the cement mortar.

The governing equations for the composite PCM-CM layer are given by:

– Cement mortar:

$$\left(1-\varepsilon\right)\left[\frac{\partial H_i}{\partial t} = \nabla\left(k_i \nabla T\right)\right] \tag{2}$$

– PCM:

$$\varepsilon\left(1-\varepsilon\right)\left[\frac{\partial H_i}{\partial t} = \nabla\left(k_i \nabla T\right)\right] \tag{3}$$

where ε being the PCM volume fraction in the cement mortar, and H is the total volumetric enthalpy, which is splitted into sensible and latent enthalpies as eq. (4).

$$H_i = h_i + \rho_{\mathrm{PCM}} f L \tag{4}$$

where f is the volume fraction of the liquid, ρ_{PCM} – the density of PCM, and L – the latent heat of PCM. The sensible enthalpy h can be given in terms of the temperature and the specific heat capacity by the following relationship:

$$h_i = \int_{T_{\mathrm{ref}}}^{T} \rho_i c_{P,i} \mathrm{d}T \tag{5}$$

where T_{ref} is the reference temperature.

In an isothermal phase change model, the liquid phase fraction f is defined:

$$f = \begin{cases} 1 & \text{if } T \geq T_{\mathrm{m}} \text{ (liquid)} \\ 0 & \text{if } T < T_{\mathrm{m}} \text{ (solid)} \end{cases} \tag{6}$$

where T_{m} being the melting temperature of PCM.

Still in the 1-D context, the enthalpy based approach can be expressed:

$$\frac{\partial h_i}{\partial t} = \nabla\left(\alpha_i \nabla h_i\right) - \rho_{\mathrm{PCM}} L \frac{\partial f}{\partial t} \tag{7}$$

where α_i [$\mathrm{m^2s^{-1}}$] is the thermal diffusivity.

It may be pointed out that here the solid/liquid PCM interface is not tracked explicitly, and the liquid fraction evolution is usually used to handle the phase change latent and phase change interface evolution.

Initial and boundary conditions

The initial (I) and the boundary conditions (BC) for the computation domain are required to solve eq. (7). The initial condition was the uniform temperature for multi-layered wall systems. Figure 2(b) depicts the BC incorporated into the model. The associated BC are given as following.

The outer side of the wall system is subjected to a forced convection BC, with $h_{\mathrm{out}} = 19\ \mathrm{Wm^{-3}K^{-1}}$, which is expressed:

$$-k_i \left.\frac{\partial T}{\partial x}\right|_{x=0} = h_{\mathrm{out}}\left(T_{a,\mathrm{out}} - T_{w,\mathrm{out}}\right) \tag{8}$$

where the *out* indice indicates the external environment. In addition, h_{out} [$\mathrm{Wm^{-2}K^{-1}}$], $T_{w.\,\mathrm{out}}$ [K], and $T_{a.\,\mathrm{out}}$ [K] are the outside convective heat transfer coefficients, outer surface, and outdoors air temperature, respectively.

In the current work, the outdoor temperature fluctuation is described using a sine function of time as:

$$T_{a,\mathrm{out}} = 28 + 12\sin(\varpi t) \tag{9}$$

where t is the time and $\varpi = 2\pi/\tau$, τ being the period (here 24 hours).

The cooling set-point of the indoor air temperature was kept at a constant temperature $T_{a,\mathrm{in}} = 23\ ^{\circ}\mathrm{C}$. At the interior surface, a free convection BC with h_{in} (= $9\ \mathrm{Wm^{-2}K^{-1}}$) is imposed, and the BC is given:

$$-k_i \left.\frac{\partial T}{\partial x}\right|_{x=x_3} = h_{\text{in}}(T_{w,\text{in}} - T_{a,\text{in}}) \tag{10}$$

where the subscript *in* denote the PCM-CM indoor environment. Moreover, h_{in}, $T_{w.\text{in}}$, and $T_{a.\text{in}}$ are the inside convective heat transfer coefficients, inner surface, and indoors air temperature, respectively.

The initial temperature of the domain is $T(x, 0) = T_{\text{init}} = 23$ °C. As for the horizontal sides, they are assumed to be insulated.

For surfaces exposed to the inside air ($x = x_3$), the heat flux is calculated to study the effect of the PCM on the heat flow from outdoor space, and it is defined:

$$\varphi_{\text{in}} = h_{\text{in}}(T_{w,\text{in}} - T_{a,\text{in}}) \tag{11}$$

Computational procedure

To numerically solve eq. (7) along with the appropriate BC, a finite volume method (FVM) is used. Thereby, the algebraic set takes the following form:

$$a_P h_P = -(a_E h_E + a_W h_W) + h_P^{\text{old}} + \rho L(f_P^{\text{old}} - f_P^k) \tag{12}$$

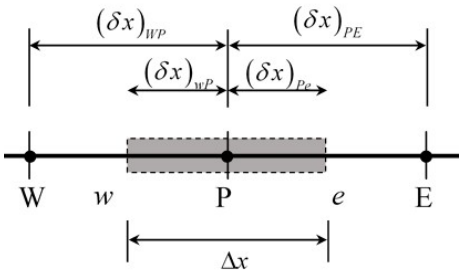

Figure 3. The 1-D finite volume stencil

The nodes *P*, *E,* and *W* being the center, east and west of the control volume, respectively, see fig. 3. The f_P^k is the k^{th} evaluation of the liquid fraction, and superscript *old* refers to the old time value. Moreover, coefficients a_P, a_E, and a_W satisfy the following relationships: $a_E = a_W = = \alpha\Delta t/(\Delta x)^2$ and $\sum_{i=W,P,E} a_i = 1$.

It should be noted that, at the interface *e*, the effective thermal conductivity is computed using relationship (13) [9]:

$$k_e = \frac{2k_E k_P}{k_E + k_P} \tag{13}$$

where k_P and k_E being thermal conductivities at nodes *P* and *E*, respectively.

Accordingly, at iteration $n+1$, the following relationship is obtained:

$$0 = -a_E h_E - a_W h_W + h_P^{\text{old}} + \rho L(f_P^{\text{old}} - f_P^{n+1}) \tag{14}$$

To track the phase change front, the needful liquid fraction is obtained by subtracting the eq. (14) of eq. (12). Thereby, the liquid fraction is updated using eq. (15):

$$f_P^{n+1} = f_P^n + \frac{\omega a_P h_P}{\rho L} \tag{15}$$

where ω is an appropriate under-relaxation factor.

During computations, the correction eq. (15) is applied to all the points by imposing a second correction for the remaining points with a liquid fraction outside [0, 1]. Once the corrected liquid fraction, the following constraint must to be satisfied:

$$f_P = \begin{cases} 0 & \text{if} \quad f_P^{k+1} < 0 \\ 1 & \text{if} \quad f_P^{k+1} > 1 \end{cases} \tag{16}$$

After implementation of all coefficients at each node, eq. (12) is iteratively solved using the well-known tri-diagonal matrix algorithm (TDMA) [23]. Recall that the liquid fraction is updated at every time step. Otherwise, the solution process is repeated until a fixed convergence criterion is met since the problem is unsteady.

Note that here, at each new time step, the updating of the enthalpy is performed until the following convergence criterion $|H_P^n - H_P^{n+1}|/\rho c_p < \tilde{\varepsilon}$ is satisfied (here $\tilde{\varepsilon} = 10^{-4}$), $\tilde{\varepsilon}$ being a prescribed tolerance. A mesh sensitivity test was carried out to examine the mesh independence of the numerical results. To insure this independence, we opted for a tight mesh on extremities and a time step of 1 second. A 100-node grid has been proved accurate for convergent solutions with compromise on enough accuracy and CPU-time consumption.

Results and discussion

Model validation

Before presenting and commenting on our main findings, the model considered has been validated beforehand by comparing simulation results to experimental data obtained coming from the guarded hot plates method. In addition, our in-house code has already been validated [17, 24]. Note that the sample examined here is the same as that which has been experimentally studied in [7] whose results were used for validation.

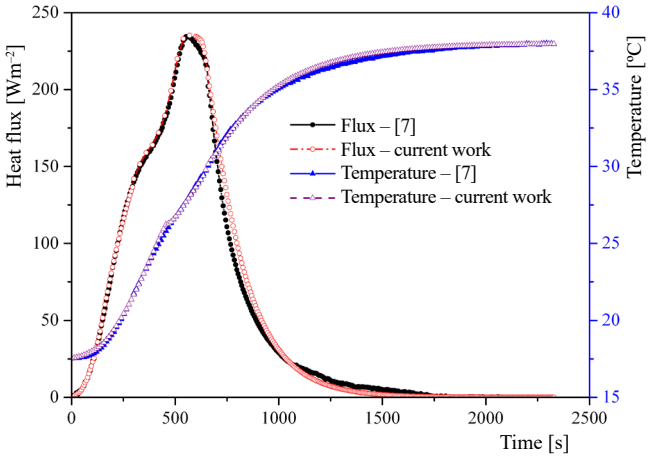

Figure 4. Temporal variation of Mortar-PCM heat flux and temperature

Experimental and numerical results of heat fluxes and temperature evolution on both sides of the composite sample, when the plaster-PCM composite follows a complete melting process, are depicted in fig. 4. From this figure, we can state that our numerical findings corroborate available data indicating that the model chosen is proper. Note that the sample is initially isothermal at a temperature T_{init} = 17 °C, fig. 4, and at a particular time, a temperature variation was imposed, while another thermal steady state is obtained at T_{end} = 38 °C. Thereby, heat fluxes evolve sharply at the beginning to reach a constant value indicating the achievement of the stable state at the end of the test. Then, the latent heat is set by subtracting the sensible heat from the total heat. Numerical and

Table 2. Numerical and experimental amounts heat stored by the Plaster/Micronal (90/10)

Plaster/Micronal90/10	Experimental [kJkg^{-1}]	Numerical [kJkg^{-1}]	Difference [%]
Total heat	20.21	20.79	2.78
Latent	14.47	15.16	4.76

experimental results obtained from total and latent heat stored by the composite-PCM during the melting cycle are gathered in tab. 2. Furthermore, it may be noted that numerical simulations of heat flux and temperature corroborate experiments herein achieved, thereby implying the reliability of the current numerical method.

Brick walls thermal behavior with a sinusoidal outside temperature variation

Based on this numerical method, a parametric study is performed to highlight significant factors that govern the performance of PCM incorporation in building envelopes. Among these factors, one can cite the phase change temperature, the thickness of the PCM-mortar composite layer and the PCM amount. Note that here, the PCM-mortar composite's effect is assessed on two walls test (W2 and W3), the wall without PCM (W1) being the reference wall.

The envelope performance was simulated using a sinusoidal the outdoor temperature variation translating the daily variation of the summer temperature, eq. (9) and constant internal BC (cooling season 23 °C). The performance assessment of the PCM incorporation is based on three ingredients, viz., seasonal peak load shifting, peak cooling loads reduction, and total annual cooling load reduction. Note that peak load shifting is the PCM layer ability to shift the peak load to another time of day, while peak load reduction serves to reduce the maximum cooling load in a given diurnal period.

The temperature values obtained on the wall's inside surface show the one of the positive effects of the PCM incorporation as an indoor temperature thermo-regulator. Figure 5 depicts the temperature profiles obtained on the inside surfaces of walls W1 and W2. The internal surface temperatures variation of the two these walls (with 20% of microencapsulated paraffin) for two 24 hours cycles are also shown. Four zones can be identified: 1 and 3 emphasize the time delay between the maximum and minimum outside temperature and the obtained temperature on the inside surface of the wall sample without PCM, while zones 2 and 4 depict the time delay between the maximum and minimum temperature obtained at the interior surface for both samples, with and without PCM incorporation. During the charging process, the time delay of the minimum load for the wall sample (without PCM) is nearly 4 hours, and is nearly 3 hours for the wall sample with PCM compared to that without PCM. On the other hand, in the discharge process (nocturnal cooling), the maximum load delay for the wall sample (without PCM) is about 4 hours and is about 2.5 hours for the wall sample with PCM compared to that without PCM. Figure 5 points out clearly the PCM effect on temperature attenuation in the wall. Note that the thermal amplitude is reduced from approximately 13 °C for wall W1 (without PCM) to 2.5 °C for wall W2 (with PCM), corresponding to a 20% of thermal amplitude reduction. In addition, the PCM incorporation attenuates the maximum and minimum temperature peaks of 2.5 °C in comparison to the wall without PCM.

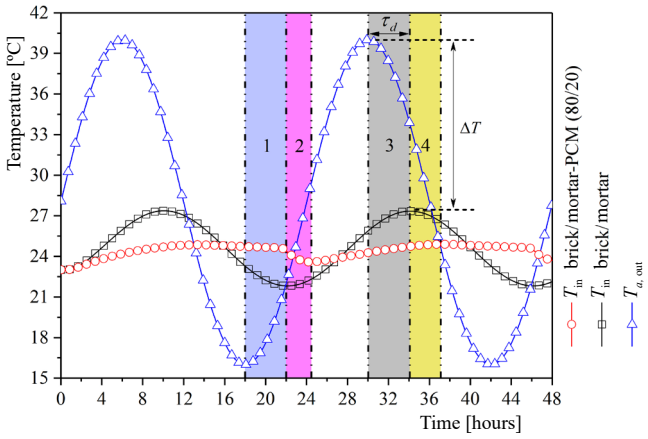

Figure 5. Temporal variation of temperature at W1- and W2-walls inner surface

The simulated heat flux variation during charging and discharging processes at inner surfaces of wall samples (W1 and W2) are shown in fig. 6. It is noted that the wall sample incorporating 20% of the PCM reduces peaks of heat flux by more 55% in comparison to the wall without PCM. In this case, the PCM acts as an insulating material that reduces heat transfer. Through what has just been quoted, the role (attenuation of temperature fluctuations inside buildings) of PCM integration becomes clear. Already, it can be stated that such a material may be useful in preventing overheating during summer. To go even further, it would be sound to conduct in-depth investigation dealing with the impact of the amount PCM and wallboard thickness on the building temperature regulation.

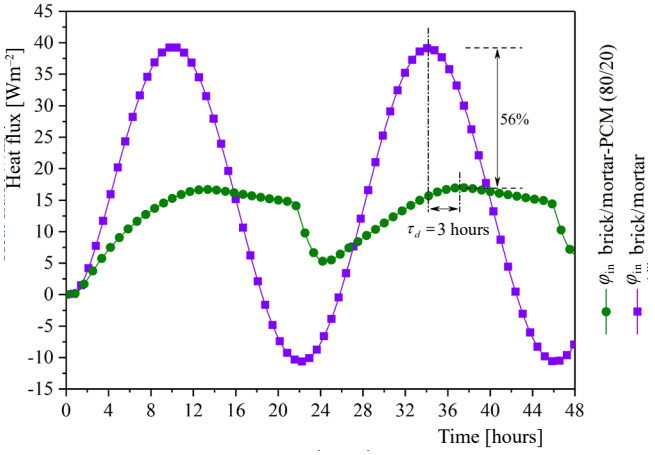

Figure 6. Temporal variation of heat flux at wall samples' inner surface

Effect of the amount of PCM amount's effect

Here we mainly seek the effect of the microencapsulated PCM amount in the mortar layer with a stabilized temperature between 23 °C and 25 °C in the construction space. For this aim, a numerical simulation was conducted during a summer day. Thereby, we studied brick walls with a mortar layer incorporating PCM micro-capsules ranging from 10% to 30%. Figures 7(a) and 7(b) show the temporal variation of average temperature and heat flux at the inner surfaces of the wall during the charging and discharging processes for a PCM volume fraction ranging from 0% to 40%. As shown, increasing the PCM volume fraction significantly reduces heat transfer through the wall while damping temperature oscillations. In other words, the internal wall heat flux decreases by more than 70% when the micro-encapsulated PCM mass fraction

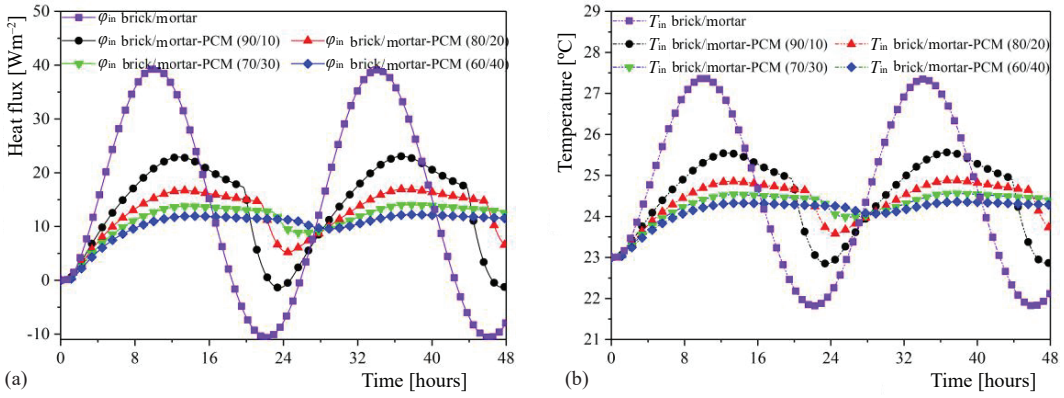

Figure 7. (a) heat flux and (b) temperature variation *vs.* time

exceeds 40%. We also note that a fraction of PCM greater than 30% does not significantly improve the attenuation of the amplitude of temperature oscillations on the inner surface of the brick wall. In other words, the composite 70/30 exhibits the same behavior as the 60/40. Indeed, it has been observed, fig. 7(a), that the temperature amplitude of the inner surface is reduced by 1.8 °C, 2.5 °C, 2.8 °C, and 3 °C for 10%, 20%, 30%, and 40% in terms of mass fraction in comparison to the wall W1 (*i. e.* without PCM). Thus, the stored heat amount increases relative to the wall sample without PCM with the PCM mass fraction. Therefore, heat transfer to the

Table 3. Maximum and minimum amplitudes of the inner surface temperature

Material	Brick/Mortar-PCM				Brick/Mortar
	90/10	80/20	70/30	60/40	
$T_{out,\,min}$	16	16	16	16	16
$T_{in,\,min}$	22.8	23.6	24	24.1	21.8
ΔT	6.8	7.6	8	8.1	5.8
$T_{out,max}$	40	40	40	40	40
$T_{in,max}$	25.6	24.9	24.6	24.4	27.3
ΔT	14.4	15.1	15.4	15.6	12.7

indoor atmosphere is reduced provided that the PCM amount required for efficient storage is between 20% and 30%.

Table 3 displays the amplitude of inner and outer surface temperatures in the case of a brick/mortar-PCM (with a different mass fraction of micro-encapsulated PCM) compared to a brick/mortar without PCM. Likewise, it demonstrates that the difference between these amplitudes increases with the amount of PCM. It may be stated that the additional thermal mass in the building envelope system generates thermal resistance. Note that, in the paper remainder, the PCM mass fraction was set at 30%.

Phase change temperature effect

Since the phase change temperature has a paramount role in the thermal performance of the wall sample containing PCM, a numerical simulation has been conducted to investigate the phase change temperature effect on the temporal temperature variation of the wall inner surface. To achieve this, three phase change temperature of PCM, viz. 24 °C, 26 °C, and 28 °C, have been considered in summer. Results from such a simulation dealing with the average temperature and heat flux on the interior surfaces are depicted in fig. 8. It should be noted that the smoother the inner surface temperature is, the more energy (during cooling process) can be saved. It is found that the wall sample incorporating PCM having a melting temperature between 24 °C and 26 °C exhibits the smoothest temperature at the inner surface, where the difference between the maximum temperature and the minimum temperature remains very low. Since the temperature at the inner surface of the wall is close to the summer comfort temperature, it is not needful to have an extra energy to keep the room with good thermal comfort. The wall W2, with a melting temperature of 28 °C, has the greatest difference between maximum and minimum temperatures during a daily thermal cycle. In addition, the presence of PCM can act as an insulator by limiting heat from the outside environment. As shown in fig. 8, the plateau existence is due to the phase change process indicating that the PCM-mortar layer temperature is stabilized around its phase change temperature during the phase transition. The lower the

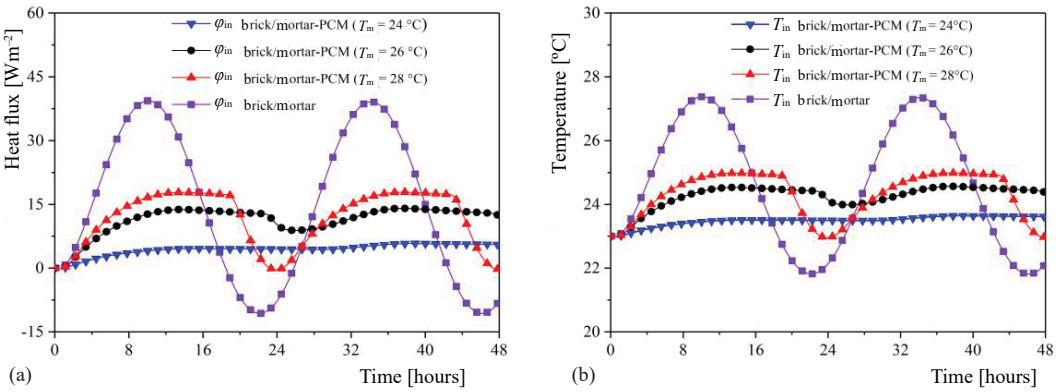

Figure 8. Inner surface heat flux and temperature variation *vs.* time

Table 4. Maximum and minimum amplitudes of the inner surface temperature for different PCM melting temperatures

	Brick/Mortar (without PCM)	T_m = 24 °C	T_m = 26 °C	T_m = 28 °C
$T_{out,min}$	16	16	16	16
$T_{in,min}$	21.8	23.5	24	23
ΔT	5.8	7.5	8	7
$T_{out,max}$	40	40	40	40
$T_{in,max}$	27.3	23.6	24.6	25
ΔT	12.7	16.4	15.4	15

melting temperature than the average outside temperature and is closer to the inner comfort temperature, the longer the plateau. This keeps both indoor thermal comfort and energy saving.

Regarding the results gathered in tab. 4, it can be stated that the melting temperature of 24 °C increases the difference between the amplitude of inner and outer surface temperatures while ensuring a peak temperature lower than that observed with melting temperatures of 26 °C and 28 °C. We note that the least temperature amplitude was observed when the PCM had a phase change temperature of 28 °C. This is because the phase change temperature is close to the average outside temperature. Thereby, the PCM with a phase change temperature of 28 °C does not have sufficient time to thoroughly change phase, and latent heat is not utilized properly to reduce the envelope heat gains. A phase change temperature greater than 26 °C does not allow a full melting-freezing cycle, and does not improve the PCM-mortar layer efficiency. In light of results thus obtained, it can be stated that a selection of PCM with a suitable phase change temperature for assuring a building cooling load reduction during a hot climate is vital.

Comparison of micronal mortar/wallboard performance with another class of wallboard

Figure 9 shows the heat and temperature flux profiles on the sample wall inner surface during charging and discharging processes. Three wall samples, viz., W1 (a brick wall without PCM), W2 (a brick masonry wall with a micro-encapsulated PCM), and W3 (a mixture layer (mortar including a PCM) with a thickness 2 cm and 10 cm of brick glued to an insulation material XPS of 10 cm thick) have been investigated, while keeping the remaining parameters unchanged from those used in the previous section (*i. e.* T_m = 26 °C, mass fraction of *PCM* = 30%). These results highlight that the inner surface temperature and heat flux for W2

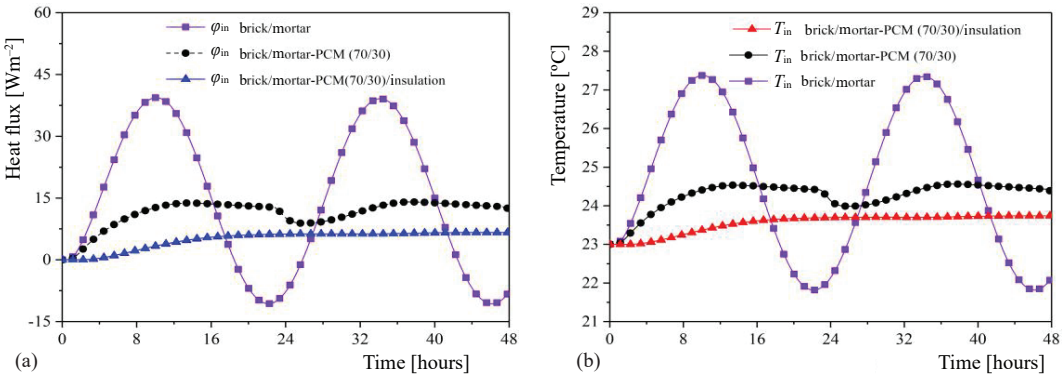

Figure 9. Inner surface heat flux and temperature variation *vs.* time

Table 5. Maximum and minimum inner and outer surface temperature for the different cases

	Brick/Mortar	Brick/Mortar-PCM (70/30)	Brick/Mortar-PCM (70/30)/Insulation
$T_{out,min}$	16	16	16
$T_{in,min}$	21.8	24	23.7
ΔT	5.8	8	7.7
$T_{out,max}$	40	40	40
$T_{in,max}$	27.3	24.6	23.8
ΔT	12.7	15.4	16.2

and W3 walls have smaller amplitudes compared with a PCM-free wall. Note that temperature variation amplitudes of W1- and W2-walls are almost identical. In addition, it is found that the wall insulation incorporating PCM reduces peaks in outdoor heat flux and to stabilize the indoor temperature. Moreover, a significant heat gain reduction of 83% is achieved by adding an XPS insulation material of 10 cm thick to wall W2. It turns out that the presence of PCM leads to temporal shift oscillations. Note that the result raised is threefold: the maximum outside temperature was 40 °C, the wall W2 with PCM had a maximum temperature of 2.5 °C lower than that of W1 and a minimum temperature of 2.2 °C higher, tab. 5; the thermal performance improvement of the W2 wall reduced its temperature by 0.8 °C, and stabilized the temperature at 23.5 °C, thus, the outside temperature variation has no effect on the internal surface temperature of the W3 wall; and the maximum temperature in the wall with PCM appears approximately 3 hours later than without PCM, indicating that the wall thermal inertia is higher. Note that the addition of an insulating layer both let to improve and preserve the thermal inertia effect provided by the PCM. It sounds that the low polystyrene thermal conductivity and the high PCM heat storage capacity are key parameters that allow a maximum load reduction and load shifting.

Conclusion

The current study targeted the thermal performance analysis of brick masonry walls incorporating a PCM for passive cooling. To achieve this aim, an enthalpy-porosity model has been implemented in an in-house code to handle phase change process. Beforehand, we validated this approach by comparing our results with experimental data from the guarded hot plates method. To determine the wall optimal design, several simulations have been performed for different parameters of interest. The main outcomes of this study are as follows.

- Combination of a PCM mortar layer and a brick wall was found to be suitable to reduce cooling peaks, and to successfully shift cooling peaks in final hours of the day, while significantly reducing heat transfer.
- The PCM incorporation helped to absorb the heat resulting from external thermal conditions, thereby attenuated the indoor temperature, reducing the thermal amplitude from 3 °C and increasing the delay of about 3 hours, thereby pointing that the thermal inertia of the wall is higher.
- The PCM should have a low phase change temperature to maintain the surface temperature at a low level, but high enough to ensure a full melting-freezing cycle.
- Increasing the PCM amount incorporated into masonry enclosure walls leads to an improved thermal inertia and reduced greatly the heat flux amplitude and temperature oscillations. Hence, these findings can be a real opportunity for energy savings in buildings via PCM incorporation into brick walls.

Nomenclature

c_p – specific heat, [Jkg^{-1}K^{-1}]
f – liquid fraction, [–]
H – total enthalpy, [Jm^{-3}]
h – specific enthalpy, [Jm^{-3}K^{-1}]
k – thermal conductivity, [Wm^{-1}K^{-1}]
L – latent heat of fusion, [Jkg^{-1}]
m – total mass [kg]
T – temperature, [K]
T_a – air temperature, [K]
T_m – melting point of materials, [K]
T_w – wall temperature [K]
t – time, [s]
x – component in x-direction [m]

Greek symbols

φ – heat flux, [Wm^{-2}]
ω – relaxation factor, [–]
ρ – density, [kgm^{-3}]
τ – period, [second or hour]

Superscripts/subscripts

end – final
E, P, W – east, center and west
ini – inside
init – initial
m – melting
old – old time value

References

[1] Soares, N., *et al.*, Review of Passive PCM Latent Heat Thermal Energy Storage Systems Towards Buildings' Energy Efficiency, *Energy and Buildings*, *59* (2013), Apr., pp. 82-103
[2] Dong, L., *et al.*, Numerical Analysis on Thermal Performance of Roof Contained PCM of a Single Residential Building, *Energy Conversion and Management*, *100* (2015), Aug., pp. 147-156
[3] Shazim, A. M., Phase Change Materials Integrated in Building Walls: A State of the Art Review, *Renewable and Sustainable Energy Reviews*, *31* (2014), Mar., pp. 870-906
[4] Lucas, S. S., *et al.*, Latent Heat Storage in PCM Containing Mortars Study of Microstructural Modifications, *Energy and Buildings*, *66* (2013), Nov., pp. 724-731
[5] Selka, G., *et al.*, Dynamic Thermal Behavior of Building Using Phase Change Materials for Latent Heat Storage, *Thermal Science, 19* (2015), 2, pp. 603-613
[6] Vicente, R., Silva, T., Brick Masonry Walls with PCM Macrocapsules: An Experimental Approach, *Applied Thermal Engineering*, *67* (2014), 1-2, pp. 24-34
[7] Karkri, M, *et al.*, Thermal Properties of Smart Microencapsulated Paraffin/Plaster Composites for the Thermal Regulation of Buildings, *Energy and Buildings*, *88* (2015), Feb., pp. 183-192
[8] Toppi, T., Mazzarella, L., Gypsum Based Composite Materials with Micro-Encapsulated PCM: Experimental Correlations for Thermal Properties Estimation on the Basis of the Composition, *Energy and Buildings*, *57* (2013), Feb., pp. 227-236
[9] Su, J. F., *et al.*, Fabrication and Properties of Microencapsulated-Paraffin/Gypsum-Matrix Building Materials for Thermal Energy Storage, *Energy Conversion and Management*, *55* (2012), Mar., pp. 101-107
[10] Zhang, H., *et al.*, Preparation and Thermal Performance of Gypsum Boards Incorporated with Micro-Encapsulated Phase Change Materials for Thermal Regulation, *Solar Energy Materials and Solar Cells*, *102* (2012), July, pp. 93-102

[11] Oliver, A., Thermal Characterization of Gypsum Boards with PCM Included: Thermal Energy Storage in Buildings through Latent Heat, *Energy and Buildings*, *48* (2012), May, pp. 1-7
[12] Zwanzig, D. S., *et al.*, Numerical Simulation of Phase Change Material Composite Wallboard in a Multi-Layered Building Envelope, *Energy Conversion and Management*, *69* (2013), May, pp. 27-40
[13] Jaworski, M., *et al.*, Numerical Modelling and Experimental Studies of Thermal Behavior of Building Integrated Thermal Energy Storage Unit in a Form of a Ceiling Panel, *Applied Energy*, *113* (2014), Jan., pp. 548-557
[14] Kong, X., *et al.*, Numerical Study on the Thermal Performance of Building Wall and Roof Incorporating Phase Change Material Panel for Passive Cooling Application, *Energy and Buildings*, *81* (2014), Oct., pp. 404-415
[15] Castell, A., *et al.*, Experimental Study of Using PCM in Brick Constructive Solutions for Passive Cooling, *Energy and Buildings*, *42* (2010), 4, pp. 534-540
[16] Kong, X., *et al.*, Experimental Research on the Use of Phase Change Materials in Perforated Brick Rooms for Cooling Storage, *Energy and Buildings*, *62* (2013), July, pp. 597-604
[17] Younsi, Z., *et al.*, Numerical Investigation of Transient Thermal Behavior of a Wall Incorporating a Phase Change Material Via a Hybrid Scheme, *Int. Communications in Heat and Mass Transfer*, *78* (2016), Nov., pp. 200-206
[18] Lei, J., *et al.*, Energy Performance of Building Envelopes Integrated with Phase Change Materials for Cooling Load Reduction in Tropical Singapore, *Applied Energy*, *162* (2016), Jan., pp. 207-217
[19] Koo, J., *et al.*, Effects of Wallboard Design Parameters on the Thermal Storage in Buildings, *Energy and Buildings*, *43* (2011), 8, pp. 1947-1951
[20] Silva, T., *et al.*, Experimental Testing and Numerical Modelling of Masonry Wall Solution with PCM Incorporation: A Passive Construction Solution, *Energy and Buildings*, *49* (2012), June, pp. 235-245
[21] Sassine, E., *et al.*, Frequency Domain Regression Method to Predict Thermal Behavior of Brick Wall of Existing Buildings. *Applied Thermal Engineering*, *114* (2016), Mar., pp. 24-35
[22] Voller, V. R., Cross, M., *Application of Control Volume Enthalpy Methods in the Solution of Stefan Problems*, Computational Techniques in Heat Transfer, Pineridge Press, Swansea, UK, 1985, pp. 245-275
[23] Patankar, S. V., *Numerical Heat Transfer and Fluid Flow,* Hemisphere Publishing Corporation, New York, USA, 1980
[24] Younsi, Z., Naji, H., A Numerical Investigation of Melting Phase Change Process Via the Enthalpy-Porosity Approach: Application to Hydrated Salts. *Int. Communications in Heat and Mass Transfer*, *86* (2017), Aug., pp. 12-24

Paper submitted: March 2, 2018
Paper revised: July 12, 2018
Paper accepted: July 16, 2018